Nonsymmetric Holmboe instabilities in arrested salt-wedge flows

A. J. K. Yang, E. W. Tedford and G. A. Lawrence

Departments of Civil Engineering
University of British Columbia, Vancouver, BC V6T1Z4, Canada

Abstract

A salt wedge is set up in a laboratory flume and the resulting Holmboe instabilities are investigated. Particle image velocimetry and laser induced fluorescence are used to obtain velocities and the height of the density interface. The positive and negative wave modes are separated by the 2D Fourier transform. Three different instability regions with positive and negative modes are found at the salt wedge interface. Theoretical results obtained from the Taylor-Goldstein equation are compared with the observed instabilities. In the analysis, upper and lower boundaries are included and the density interface is displaced vertically with respect to the center of the shear layer. The negative instabilities are smaller in amplitude than the positive instabilities due to the bottom boundary. The theoretical predictions agree with the experimental observations.

Introduction

When considering the possibility of turbulence production and mixing in a sheared density stratified environment, it is important to determine whether or not a particular flow configuration represents a stable solution of the equation of motion. We are interested in the stability of a statically stable stratified shear flow whose density interface is much thinner than the shear layer thickness. Such background flows occur in many physical situations, for example, salt wedge flows [6] & [8] and exchange flows [7]. Most previous work is based on the assumption that the flow is unbounded. However, in many flows [8], the shear layer thickness is a significant proportion of the total flow depth. Symmetric Holmboe instabilities have been largely studied for few decades [4]. While, the asymmetry with a displacement between the center of shear layer and density interface is much more likely to occur in nature. In this paper, we will investigate the effects of finite flow depth with asymmetry.

Here, we study the stability of the inviscid flow and use the traditional method of linear stability analysis. Although linear analysis is only valid for a very short time before the nonlinear effects become important, it does correctly describe the onset and early evolution of infinitesimal perturbations, and generally gives a qualitatively correct indication of overall stability of the flow. In addition, experimental results indicate that linear stability analysis correctly predicts the wave number of unstable modes [5].

Linear stability analysis

We examine the stability of a two-dimensional (2D) inviscid flow with two layers of constant densities and with an interfacial layer of constant horizontal shear as shown in figure 1. Though the piecewise profiles are highly idealized, they are sufficient to capture the essential instability mechanisms that are present in the more realistic smooth profiles [1] and [5]. Asymmetry and boundaries are assessed in this stability study. The asymmetry refers to displacement between the center of the shear layer and the density interface denoted by $d \neq 0$. The effect of the upper and lower boundaries on the instability is included.

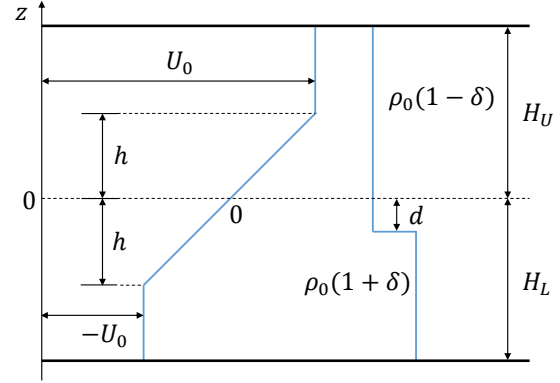First, we nondimensionalize the problem using the length, ve-

Figure 1: Definition diagram for the piecewise linear approximations of the velocity and density profiles

locity and density scales h, U_0, and ρ_0. The background density and velocity profiles are expressed as

$$\bar{u}(z) = \begin{cases} 1, & 1 < \zeta < H_u \\ \zeta, & -1 < \zeta < 1 \\ -1, & -H_l < \zeta < -1 \end{cases} \quad (1)$$

$$\bar{\rho}(z) = \begin{cases} 1-\delta, & z \geq \varepsilon \\ 1+\delta, & z < \varepsilon \end{cases} \quad (2)$$

where $\zeta = z/h$, $\varepsilon = d/h$, $\bar{\rho} = \rho/\rho_0$, and $\bar{u} = \overline{U}/U_0$ represent non-dimensional height, density, and velocity, and ε is the asymmetric parameter, whose absolute value is assumed to be less than unity. The upper and lower layer depths are nondimensionalized as $H_u = H_U/h$ and $H_l = H_L/h$.

For an inviscid flow with small variations in density, the linear stability of the flow is governed by the Taylor-Goldstein (T-G) equation:

$$\{(\sigma + ik\overline{U})^2[\frac{d^2}{dz^2} - k^2] - k^2 N^2 - ik\frac{d^2\overline{U}}{dz^2}(\sigma + ik\overline{U})\}\hat{w} = 0 \quad (3)$$

where k is the wave number; $\sigma = -ikc$ is the frequency; $\hat{w}(z)$ is the vertically varying amplitude of the velocity perturbation; and the buoyancy frequency is $N = \sqrt{(g/\rho)/(-d\rho/dz)}$.

From the piecewise linear profiles of density and velocity, using the techniques outlined in [2], we obtain the following non-dimensional eigenvalue equation

$$a\sigma^4 + b\sigma^3 + c\sigma^2 + d\sigma + e = 0 \quad (4)$$

where

$$a = (T_+ + \frac{1}{T_l})(1 + \frac{T_-}{T_u}) + (T_- + \frac{1}{T_u})(1 + \frac{T_+}{T_l})$$

$$b = -2i\alpha\varepsilon a + iA_-$$

$$c = \alpha^2(1-\epsilon^2)a + 2\alpha\epsilon A_- - \alpha A_+ + T_+ + T_- + 2\alpha J B$$
$$d = -2i\alpha\epsilon(\alpha^2 a - \alpha A_+ + T_+ + T_-) - i\alpha^2\epsilon^2 A_- + 2i\alpha J D_-$$
$$e = -\alpha^2\epsilon^2(\alpha^2 a - \alpha A_+ + T_+ + T_-) + 2\alpha J(\alpha^2 B - \alpha D_+ + T_+ T_-),$$

$$A_- = (T_+ + T_-)\left(\frac{1}{T_u} - \frac{1}{T_l}\right)$$
$$A_+ = 2(1 + T_+ T_-) + (T_+ + T_-)\left(\frac{1}{T_u} + \frac{1}{T_l}\right)$$
$$B = 1 + \frac{T_+}{T_l} + \frac{T_-}{T_u} + \frac{T_+ T_-}{T_u T_l}$$
$$D_- = T_+ - T_- + T_+ T_-\left(\frac{1}{T_u} - \frac{1}{T_l}\right)$$
$$D_+ = T_+ + T_- + T_+ T_-\left(\frac{1}{T_u} + \frac{1}{T_l}\right)$$

and

$$T_u = \tanh\alpha(H_u - 1), \quad T_l = \tanh\alpha(H_l - 1)$$
$$T_+ = \tanh\alpha(1 + \epsilon), \quad T_- = \tanh\alpha(1 - \epsilon)$$
$$S_u = \sinh\alpha(H_u - 1), \ldots \quad C_u = \cosh\alpha(H_u - 1), \ldots$$

All of the variables in the above equation are dimensionless: the instability wave number is $\alpha = kh$ and the Richardson number is $J = 2g'h/\Delta U^2$ (where $g' = g\Delta\rho/\rho_0$ and $\Delta U = 2U_0$). The special case, $H_u = H_l$, was examined by Haigh & Lawrence [3]. When H_u and $H_l \to \infty$, was studied by Lawrence et al. [5]. With further simplification, H_u and $H_l \to \infty$ and $\epsilon = 0$, was studied by Holmboe [4].
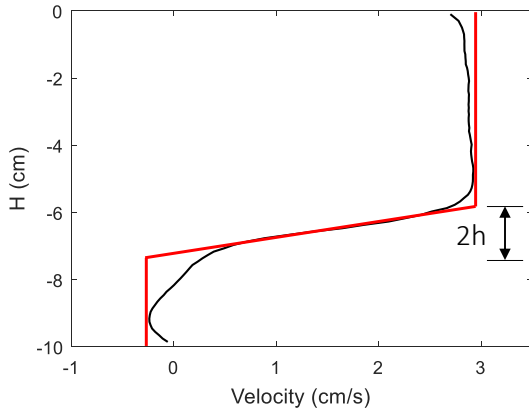

Figure 2: PIV measured velocity profile and its definition sketch for piecewise linear profiles ($x = 160$ cm)

Dispersion relation and instability

Figure 2 shows the PIV measured velocity profile and its fitted piecewise linear profile. The corresponding experimental parameters are given in table 1. The shear layer thickness is much thicker than that of the density profile, thus the density distribution is assumed to be a step function with a negligible influence on the Holmboe instability [7]. The key parameters in the stability analysis are the velocity difference between the layers ΔU, the shear layer thickness $2h$, the reduced gravity acceleration g' and the bulk Richardson number J.

In figure 3(a), the growth rate αc_i against the non-dimensional wave number for positive (red solid line) and negative (black dash line) instabilities is illustrated. The asymmetry ϵ is zero. For a given Richardson number $J = 0.4$, the growth rates of

both the positive and negative instabilities vary with the wave number. The top and bottom boundaries are far from the center of the shear layer and negligibly influence instabilities. The positive and negative instabilities are symmetric in this case. As the shear layer approaches the lower boundary (figure 3(b)), the negative instability is inhibited in terms of both the growth rate and the range of the wave number. This boundary also opens a small new positive growth rate region with a smaller value of wave number starting from 0.51. From the dispersion relation, the Holmboe instability (H) is caused by the interaction of vorticity wave (v) and internal gravity wave (g) ([1]). The interaction of lower ($c_r < 0$) v and g is weaker than that of the upper ($c_r > 0$) ones, and makes the Holmboe wave region narrower. As the influence of the bottom boundary increases (figure 3(c)), the negative instabilities almost disappear. Also, the offset $\epsilon = -0.5$ starts to play a role in the growth rate. It totally prevents the positive instabilities, which is referred as the "one-sidedness". The offset adding together the lower boundary effect makes it difficult to observe either instabilities in this region. It should be noted that the positive instability possibly occurs at a high wave number ($2\alpha > 4$), which is usually damped by viscosity in reality.

(a) $H_l = 4.0, H_u = 8.0$

(b) $H_l = 1.3, H_u = 10.7$
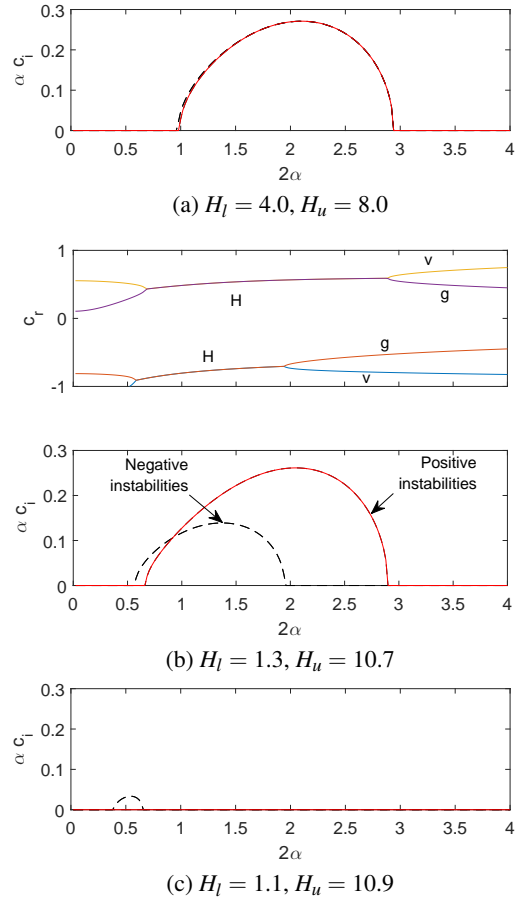

(c) $H_l = 1.1, H_u = 10.9$

Figure 3: Dispersion relation and exponential growth rate for the Holmboe flow configuration from (a) both positive and negative wave region to (b) positive wave dominant region and to (c) no wave region

Experiments

A salt wedge is set up in a laboratory flume to investigate the interfacial instabilities. A schematic of the experimental set-up of salt wedge flows is shown in figure 4(a). The dimensions of
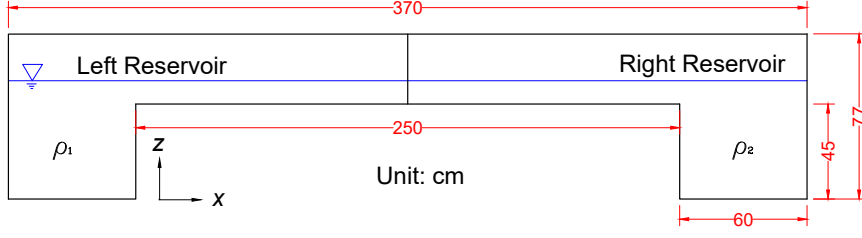
(a) Schematic of the experimental set-up of salt-wedge flows
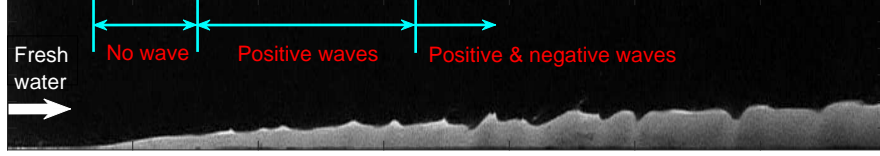
(b) Experimental observation of the typical interfacial wave regions (part of snapshot)

Figure 4: Experimental set-up (a) and observations of the typical interfacial wave regions (b)

H	L	W	g'	h	ΔU	J
(cm)	(cm)	(cm)	(cms^{-2})	(cm)	$(cm\,s^{-1})$	$(-)$
10.8	240	10	2.4	0.9	3.3	0.4

Table 1: Experimental parameters

the flume are outlined. The tank was divided into two equally sized reservoirs and connected by a 10 cm wide channel. The water was well mixed between the reservoirs to ensure uniform temperature. A gate was placed mid channel to equally divide the fluid into two equal volumes. The water temperature was $25°C$.

Laser-induced fluorescence (LIF) was used to visualize the density interface along the whole channel by illuminating fluorescein dye in the salt water (lower layer) with a continuous solid state laser (530 nm). A filter was installed in front of the LIF cameras to allow the separation of the signal with later Particle image velocimetry (PIV). A sample image is shown in figure 4(b). The interface was identified by locating the maximum vertical gradient in light intensity. PIV was used to measure the velocity of pliolite VT-L particles (Goodyear Chemical Co.).

At the start of the experiment the gate was removed and a pump placed in the salt water reservoir was switched on. The pump slowly drew water from the salt water reservoir and deposited it into the base of the fresh water reservoir. This created a flow with in the connecting channel from the fresh water (left) reservoir toward the salt water (right) reservoir. The flow enters a long period of relatively steady arrested salt-wedge flows, once the Helmholtz oscillations dampen out [7]. A total number of 12 experiments have been conducted.

In the first instance, it is beneficial to perform a simple visualization of waves at the density interface in different experiments. This is shown in figure 4(b), where a representative photograph of the laboratory waves is displayed with a sharp density interface. These waves are reminiscent of the Holmboe instability [4], which consists of positive and negative instabilities of equal growth rates and equal but opposite phase speeds [5]. The velocity shear is increasing from upstream (left) to downstream (right). In the salt wedge case, the background velocity profiles often have a displacement between the center of the shear layer and the density interface in the no wave region. On the L.H.S. of the salt wedge, a bottom boundary

layer flow with a thickness of around 3 cm is present. In the no wave region, this boundary layer results in a strongly asymmetric flow. Momentum diffusion as the fresh water flows to the right changes from this asymmetric flow to a symmetric flow in the positive wave region. As illustrated by the theory, $\varepsilon = -0.5$ (figure 3(c)), the positive wave dies down totally. Rightward of no wave region, the positive waves with upward cusps were observed; while the negative waves, which cusp toward the lower layer, can be found near the exit region. The positive and negative waves appear in different location, called "one-sidedness" phenomenon. The positive wave region is caused by the inhibition of the negative waves by the lower boundary (figure 3(b)).

Many of the basic features in the wave field are revealed by an $x - t$ characteristics diagram of the deviation of density interface elevation from its temporal mean as shown in figure 5(a). The characteristics represent a compilation of interface deviation observed in thousands of images. The dispersion relation in figure 5(b) is obtained by a 2D Frourier transform to express the interfacial elevation in the wave number-frequency plane. In the reference of the mean flow, the interface consists of contributions from both upper and lower Holmboe wave modes travelling in opposite directions. Due to the strong mean flow, both positive and negative modes travels downstream and the corresponding energy is located in the second & fourth quadrants. The positive and negative modes are separated by the mean flow (dash black line) before performing the inverse transform. The positive waves and negative waves are illustrated in figure 5(c) and (d), respectively. The speeds of the positive and negative wave are increasing due to the acceleration of the mean flow to the downstream.

Conclusions

This investigation aims to understand the generation of Holmboe instabilities in arrested salt-wedge flows. The analytical solutions of the Taylor-Goldstein equation with asymmetry and boundaries are obtained. The effects of asymmetry and upper and lower boundaries on stabilities are examined. The predicted results are compared with the experiments. Holmboe waves were observed. The 2D Fourier transform was used to separate the waves into positive and negative modes. Due to the lower boundary, the negative instabilities are smaller in amplitude than the positive instabilities. The the disappearance of positive instabilities are caused by the asymmetry (ε). With ε, the strength of positive instability is weaker.
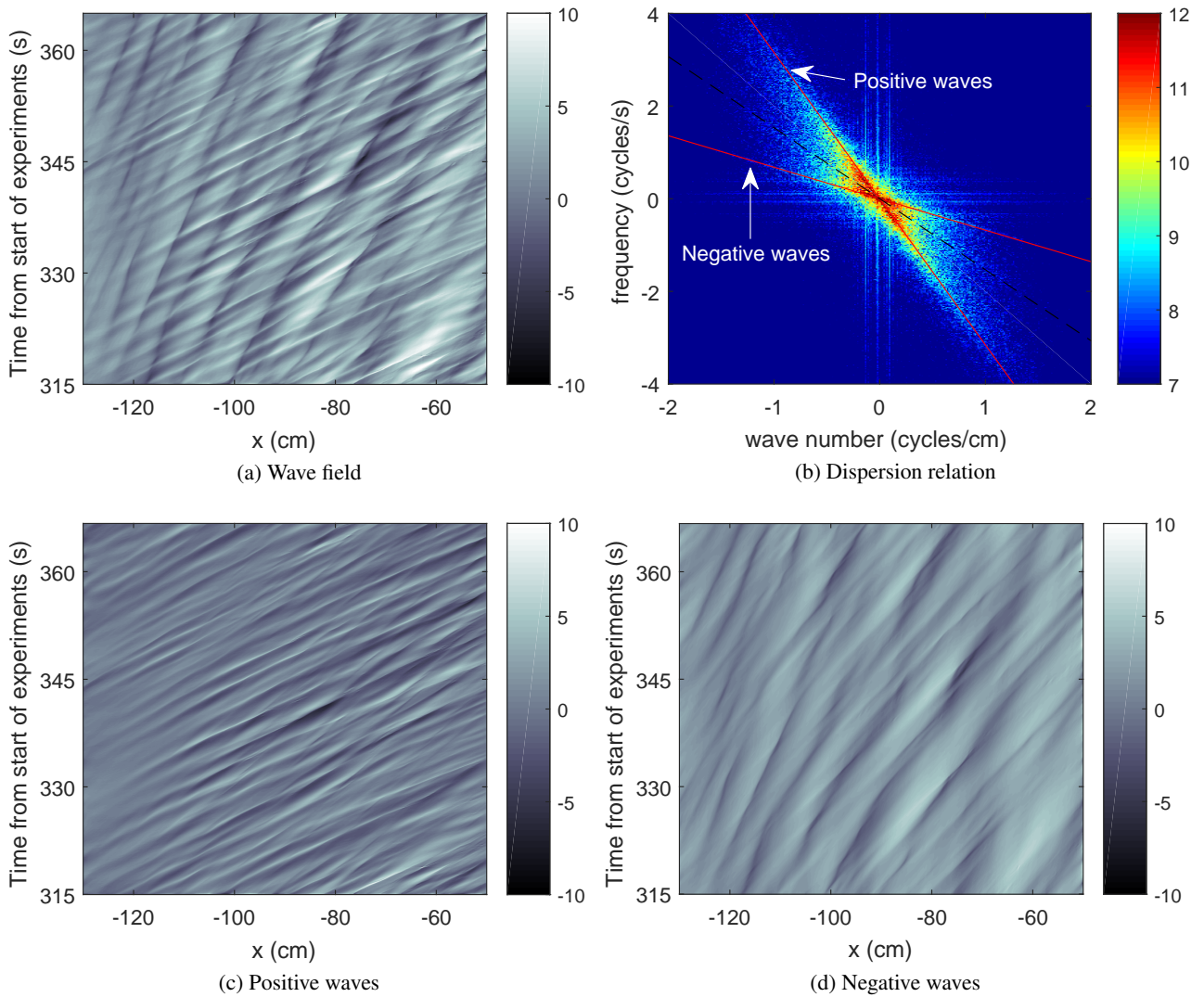
Figure 5: (a) Characteristics $(x-t)$ during the period of steady salt wedge. The shading indicates the deviation of the interface elevation from the mean. Pure white (black) indicates a positive (negative) deviation. (b) The dispersion relationship is obtained through 2D Fourier transform from characteristics. (c) The positive waves and (d) negative waves are obtained through 2D inverse Fourier transform from dispersion relation based on the black dash line in (b)

References

[1] Carpenter, J. R., Tedford, E. W., Heifetz, E. and Lawrence, G. A., Instability in stratified shear flow: Review of a physical interpretation based on interacting waves, *Applied Mechanics Reviews*, **64**, 2011, 060801.

[2] Drazin, P. G. and Reid, W. H., *Hydrodynamic stability*, Cambridge university press, 2004.

[3] Haigh, S. P. and Lawrence, G. A., Symmetric and nonsymmetric holmboe instabilities in an inviscid flow, *Physics of Fluids*, **11**, 1999, 1459–1468.

[4] Holmboe, J., On the behavior of symmetric waves in stratified shear layers, *Geofysiske Publikasjoner*, **24**, 1962, 67–113.

[5] Lawrence, G. A., Browand, F. K. and Redekopp, L. G., The stability of a sheared density interface, *Physics of Fluids A: Fluid Dynamics*, **3**, 1991, 2360–2370.

[6] Tedford, E. W., Carpenter, J. R., Pawlowicz, R., Pieters, R. and Lawrence, G. A., Observation and analysis of shear instability in the Fraser River estuary, *Journal of Geophysical Research: Oceans*, **114**.

[7] Tedford, E. W., Pieters, R. and Lawrence, G. A., Symmetric holmboe instabilities in a laboratory exchange flow, *Journal of Fluid Mechanics*, **636**, 2009, 137–153.

[8] Yonemitsu, N., Swaters, G. E., Rajaratnam, N. and Lawrence, G. A., Shear instabilities in arrested salt-wedge flows, *Dynamics of atmospheres and oceans*, **24**, 1996, 173–182.